ISABE-2013-1712

EFFECTS OF DIFFERENT PROPELLER MODELS ON OPEN ROTOR FUEL CONSUMPTION

Linda Larsson
GKN Aerospace
SE-461 81 Trollhättan, Sweden
linda.larsson@gknaerospace.com

Anders Lundbladh
GKN Aerospace
SE-461 81 Trollhättan, Sweden

Tomas Grönstedt
Chalmers University of Technology
Department of Applied Mechanics
Fluid dynamics division
SE-412 96 Göteborg, Sweden

Abstract

In this study three different ways to represent a counter rotating propeller are evaluated. One where a map for a single rotating propeller is used, one where most of the swirl losses are excluded from the original map, and one where swirl losses are excluded and the position of the maximum efficiency is determined by the design disc loading.

The two methods using the reduced swirl maps generate similar trends with similar size propellers for the optimal design and similar fuel burn figures. If the original single rotating map is used to represent counter rotating propellers the trends are significantly changed and are viewed to be unphysical. The optimal size propeller is then closer to 4.5 m rather than 3.5 meters.

With the maps where a reduction in swirl losses are accounted for, the trends show a slightly decreasing fuel consumption with decreasing tip speed. If the single rotating propeller map is used there is an opposite trend and it is of higher magnitude.

Nomenclature

C_p	Coefficient of power
CR	Counter rotating
C_t	Coefficient of thrust
D	Propeller diameter
htr	Hub tip ratio
J	Advance ratio
n	Rotational speed
P	Power
T	Thrust
U_{tip}	Propeller blad tip speed
v_0	Flight velocity
v_e	Exhaust stream velocity
η	Efficiency
η_p	Propulsive efficiency
ρ	Air density
θ	Average swirl angle

Introduction

Much of today's research and development in the aviation industry aims at reducing its environmental impact by minimizing aircraft fuel consumption. For engines one way to achieve lower fuel consumption is to increase the propulsive efficiency of the engine. One concept that is promising is the open rotor engine. The benefit of an open rotor compared to a conventional turbofan configuration is that the diameter of the propulsor can increase with comparatively less weight and drag penalty.

The open rotor engine with contra rotating propellers is not a new concept. Demonstrators have been built in the 1980s when both GE and P&W together with Allison tested the concept [1]. Although the open rotor did not reach the market in the 80s and 90s it is anew being developed within for example the European Clean Sky program in which GKN Aerospace is actively involved.

For any engine architecture it is of interest to evaluate the potential minimal fuel consumption for a certain engine type and assumed technology level. The intended aircraft application, mission and the weight of the system needs to be taken into account. To do these evaluations multidisciplinary conceptual design is often used, including aircraft modelling, engine weight modelling, mission analysis and engine performance modelling [2]. In order to model the open rotor engine concept methods and models to predict the performance of counter rotating propellers are needed. Methods used in recent studies range from using efficiency correlations based on experiments of the UDF-propellers carried out in the 80s [3], models based on single rotating propeller maps [4] or using numerical propeller design codes [5].

In this study three different ways to represent a counter rotating propeller are evaluated. The propeller performance is based on propeller data provided by Hamilton Standard found in [6]. For each of the three models studied, propeller design parameters such as disc loading and blade tip speed are varied to find the lowest fuel consumption possible for a given aircraft and mission. The different trends due to different propeller maps are explored in order to gain insight into the importance of propeller map choice.

Propeller performance basics

Propeller performance is often presented in propeller maps where the efficiency is a function of advance ratio (1) and coefficient of power (2).

$$J = \frac{v_0}{nD} \tag{1}$$

$$C_p = \frac{P}{\rho n^3 D^5} \tag{2}$$

The efficiency (3) captures how much of the shaft power that is turned into useful thrust. This means that the propulsive efficiency, swirl losses as well as profile/turbo machinery losses are included in the number.

$$\eta = \frac{T v_0}{P} = \frac{C_t J}{C_p} \tag{3}$$

$$C_t = \frac{T}{\rho n^2 D^4} \tag{4}$$

Two of the parameters often used to find the desired design is propeller blade tip speed and disc loading (5).

$$DiscLoading = \frac{P}{D^2} \tag{5}$$

For a given design point, including altitude, Mach number, disc loading and tip speed the advance ratio and coefficient of power is found using the following relations:

$$J = \frac{v_0 \pi}{u_{tip}} \tag{6}$$

$$C_p = DiscLoading \frac{J^3}{v_0^3 \rho} \tag{7}$$

Propeller map analysis

For this study performance data for the eight bladed single rotating propeller found in [6] is used as a base for further analysis. This propeller is designed for operation at 35 000 ft and Mach 0.8. Its blade tip speed in the design point is 243.8 m/s and the disc loading is 301 kW/m^2. This results in an advance ratio, J=3.06 and a coefficient of power, C_p=1.7. The hub tip ratio for the propeller is 0.25. The propeller

performance is given as different maps for different Mach numbers. One map is for Mach numbers below 0.55, the others are for Mach equal to 0.55, 0.70, 0.75 and 0.8. In Figures 1 and 2 the original propeller maps for Mach 0.8 and for low Mach numbers are shown. Since this map includes

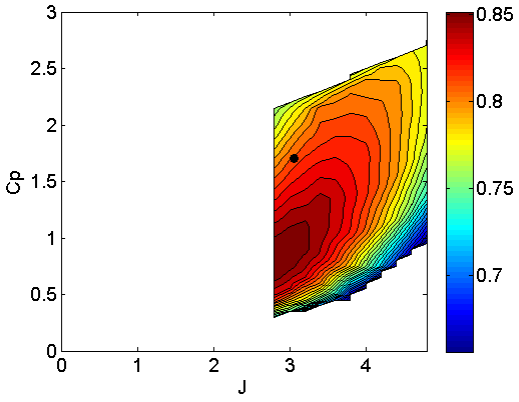

Figure 1: Original propeller performance map for Mach 0.8. Propeller efficiency for each C_p and J. The position of propeller design point is indicated.

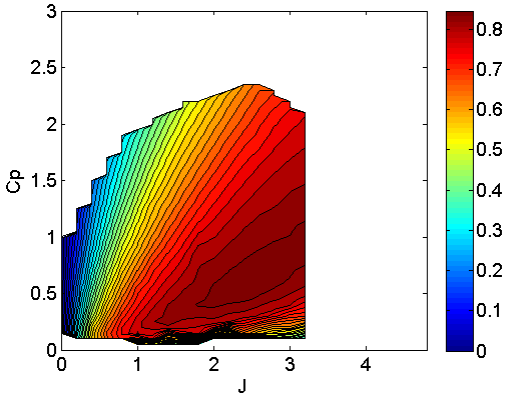

Figure 2: Original propeller performance map for low Mach numbers. Propeller efficiency for each C_p and J.

all type of propeller losses it is specific to the particular propeller design. In order to make the map more generic and representative of counter rotating propellers the propulsive efficiency and swirl losses are sought. If these loss sources can be isolated it may be possible to establish a more consistent map scaling procedure.

Loss terms

Using incompressible actuator disc theory the propulsive efficiency of the propeller can be calculated using the following relation. The derivation of the relation is given in the appendix. Using compressible actuator disc theory [7] it is found that compressible effects does not have an effect on the propulsive efficiency.

$$\eta_p = \frac{2}{1+\sqrt{1+\frac{C_t 8}{J^2\pi(1-htr^2)}}} \tag{8}$$

For the available performance data the propulsive efficiency for M 0.8 is shown in Figure 3.

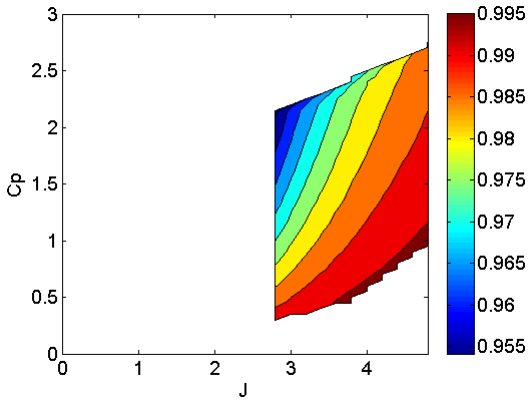

Figure 3: Propulsive efficiency for different C_p and J for Mach 0.8

Included in the data are conditions within the propeller slipstream. This data consists of average swirl angle, as seen in Figure 4, and

incremental velocity increase across the disc over free stream velocity shown in Figure 5. Using the

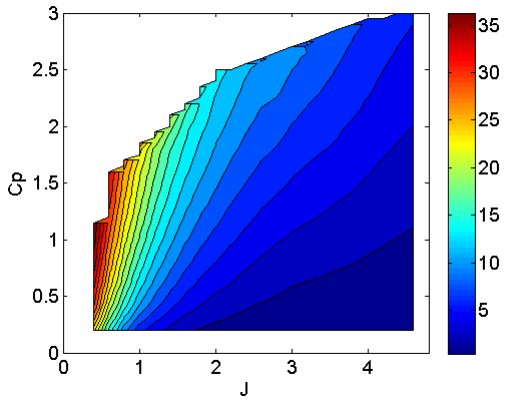

Figure 4: Average swirl angle for different C_p and J

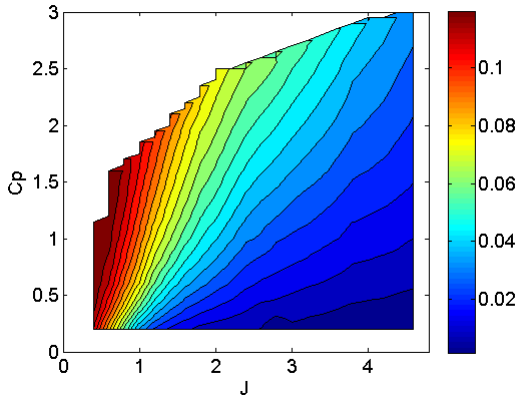

Figure 5: Incremental velocity increase over free stream velocity for different C_p and J

slip stream properties, the ratio of kinetic energy in the tangential direction over the total shaft power can be calculated. This then constitutes a measure of swirl losses. The following relation is used to calculate the swirl loss. The derivation can be found in the appendix.

$$SwirlLoss = \frac{\pi(1-htr^2)}{8}\frac{J^3(1+\frac{\Delta v}{v_0})^3\tan^2\Theta}{C_p} \quad (9)$$

The resulting swirl losses can be seen in Figure 6.

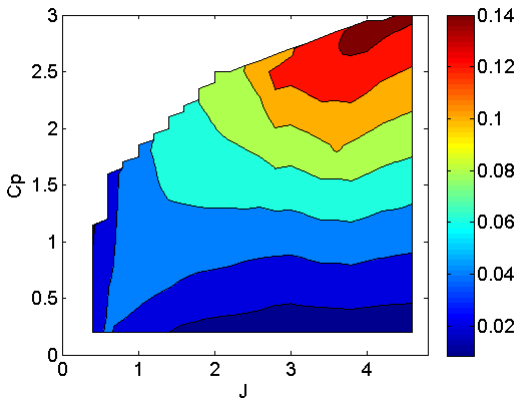

Figure 6: Swirl losses for different C_p and J

Counter rotating propeller map

In a counter rotating configuration the second propeller add more power to the slip stream and it removes most of the swirl generated by the up-stream propeller. To account for the reduced swirl, 90 % of the relative swirl losses are removed from the original map, resulting in the map shown in Figure 7.

When comparing the map with low swirl losses in Figure 7 to the map for the counter rotating F7A7 propeller configuration, as shown in Figure 8 [8], it is striking that the two maps now are similar as exemplified by the peak efficiency location. To account for the additional power added to the slip stream by the second propeller the coefficient of power needs to be scaled. The design coefficient of power for the F7A7 map is 2.68 while the coefficient for the single rotating map is 1.7. Therefore a

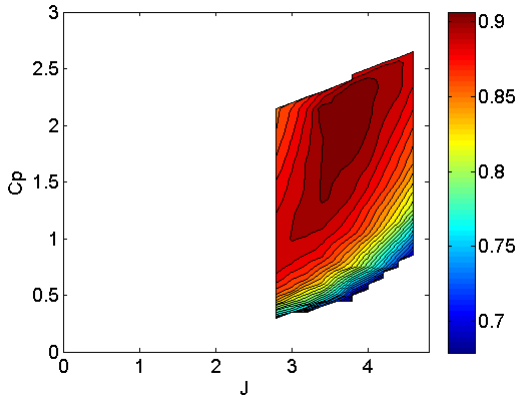

Figure 7: Resulting propeller map when 90 % of the swirl losses are removed

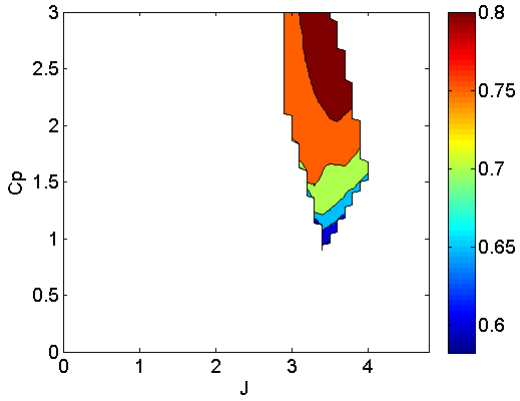

Figure 8: Propeller efficiency for the F7A7 counter rotating propeller [8]

map representative of the counter rotating propeller configuration could be modeled by multiplying the original coefficient of power by 1.58.

The study

In this paper an open rotor design that gives the minimum fuel consumption for a given aircraft and mission is sought. Three different options on how to model propeller performance have been evaluated:

1. The original unscaled propeller map from [6]
2. The propeller map modified to represent a counter rotating propeller using a fixed scaling of C_p
3. The same propeller map as in case two, but different C_p scaling depending on design disc loading and tip speed

The first two cases are equivalent to using two different existing propeller designs. This results in limitations with regard to maximum allowable C_p and J. This also means that the range of available design choices with respect to propeller diameter and rotational speed is limited. Furthermore, no account is taken for the effect of different design targets. In the third case the same shape of the propeller map is assumed as in case two, but here the scaling of C_p is changed with every choice of disc loading and propeller tip speed. The scale factor is chosen so that C_p for every disc loading corresponds to the same C_p in the original map.

Engine design point parameters such as compressor pressure ratio, core mass flow, combustor outlet temperature and component efficiencies are kept constant. The design point parameters being varied are propeller tip speed and disc loading. The aircraft studied corresponds to an aircraft of Boeing 737 size and range. The engine studied is an open rotor configuration where the power turbine is driving the two propellers via a gearbox.

Method

The mission fuel consumption is found using multidisciplinary conceptual design. Aircraft performance is found using the in house aircraft design code GISMO [9].

Engine performance is modeled using GESTPAN [10], a generic tool for gas turbine design and analysis. Conceptual design of the engine resulting in dimensions and weight is performed with a conceptual design tool called WEICO [11]. The resulting aircraft and engine is evaluated for a given mission. To vary design parameters in order to find an optimal design the commercially available integration and optimization environment ISIGHT [12] is used.

Performance maps as described above are used to calculate propeller performance. The loss due to propulsive efficiency is removed from the map. When using the map in performance calculations the propulsive efficiency is instead found using actuator disc theory. For a chosen design speed and altitude a design disc loading and propeller tip speed is chosen. From Equation 6 and Equation 7 the design J and C_p is calculated. The turbine power available in the design point then gives the needed propeller diameter and rotational speed.

When the propeller diameter and rotational speed is known, the coefficient of power and advance ratio can be calculated throughout the mission. The propeller efficiency for each point of the mission can then be found. The coefficient of thrust and propulsive efficiency is then determined using an iterative process. Finally, the propeller thrust for the available power is calculated. Propeller module weight is calculated using a function based on blade length.

Results

Original propeller map

In Figure 9 the propeller map for Mach 0.8, as used in the calculations within this section, is shown. The propeller tip speed and disc loading are varied to give different design points in the map. The position of these design points are indicated in the figure.

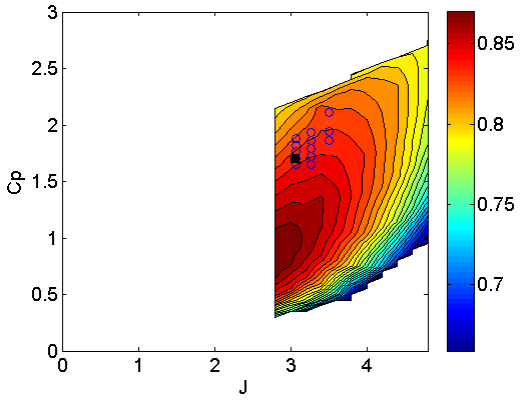

Figure 9: Original propeller map. The different design points in this study are included. The point indicated with a black marker is the original design point for the map.

Figure 10 shows the resulting mission fuel consumption for the different design points. Note that higher disc loading implies a smaller propeller diameter. Since the propeller map does not extend to very high coefficients of power there is a limit to the possible disc loading. Reduced tip speed means that the disc loading also needs to be low, otherwise C_p will increase for the given power. Thus a high J, which is equivalent to low tip speed, means a large propeller diameter. Even though the map used in this case is really more representative of a single rotation propeller it is here used as representation of a counter rotating propeller. This means that the weight of the propeller module is higher than it would be for the same diameter single propeller. Since the propeller diameter is increasing significantly with higher J the weight of the engine is increased and the resulting fuel consumption is then

increased. For the highest tip speed the fuel consumption is better for the larger propeller designs. This is due to the large penalty in efficiency when going to higher C_p, as seen from Figure 9.

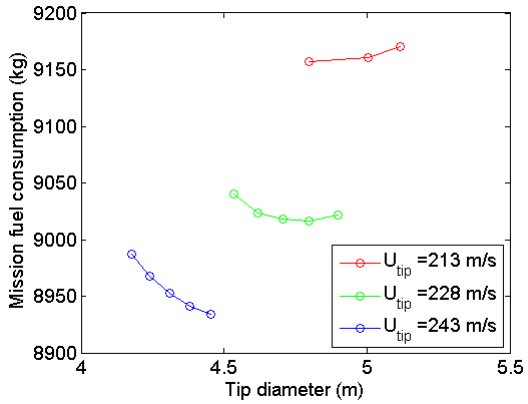

Figure 10: Fuel consumption for varying design point in original propeller map.

With a tip speed of 243 m/s the fuel consumption is 0.5 % higher with a 4.2 m propeller compared to a 4.4 m design. The fuel consumption penalty when going to a tip speed of 228 m/s is 1 %.

CR propeller map

In Figure 11 the propeller performance map representative of a counter rotating propeller is shown together with the design points evaluated for this map. In Figure 12 it can be seen that there is an optimal propeller diameter around 3.5 meters for both 243 m/s and 228 m/s propeller tip speed. For the 213 m/s propeller tip speed it is not possible to reach a fuel burn minimum since C_p will be outside the range of propeller maps for smaller diameters. When reducing the tip speed a fuel consumption decrease is observed. The fuel consumption is reduced by 0.3 % between 243 m/s to 228 m/s.

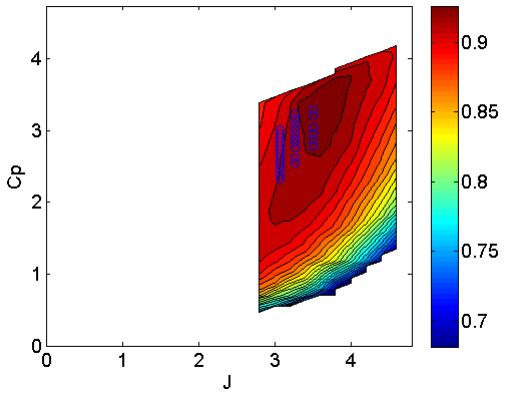

Figure 11: Propeller map representative of counter rotating propeller. The different design points in this study are included.

For the 228 m/s design tip speed the effect of increasing the diameter from the optimal 3.5 m to 4 m is a 0.4 % increase in fuel consumption.

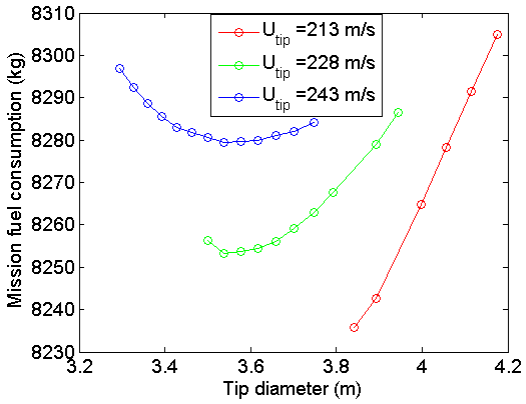

Figure 12: Fuel consumption for varying design point in the counter rotating propeller map.

CR propeller map, free scaling

In Figure 13 the position of the design point is indicated. This position is then kept constant by varying the scaling of the power

coefficient as design disc loading is being changed.

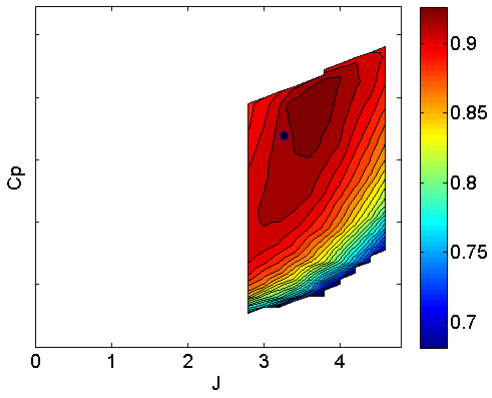

Figure 13: Propeller map representative of counter rotating propeller. The position of the design point for the free map scaling is indicated. Note that the C_p axis changes for every design point.

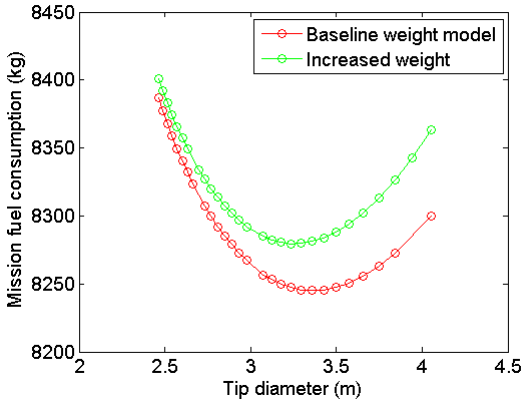

Figure 14: Fuel consumption for the free scaled map for different propeller diameters. The lower curve shows results with baseline propeller module weight model. The upper curve shows the results with 50 % increased propeller installation weight. Both curves are for 228 m/s tip speed

For the free propeller design there is a clear optimal propeller diameter as seen in Figure 14. The diameter is a trade between specific fuel consumption and engine weight. Therefore the position of the optimum is highly dependent on engine and propeller module weight. Two curves are shown where the curve with the higher fuel consumption has a 50 % higher propeller installation weight. In this sensitivity assessment, the weight of the propeller blades and gear box are unmodified but the additional installation weight is increased. The increased weight results in the optimal propeller diameter being moved to 3.2 m rather than 3.4 m. This also results in an 0.4 % higher fuel consumption. Also for this case the chosen propeller tip velocity has a some effect on mission fuel consumption. 0.2 % decrease in fuel consumption with 213 m/s rather than 228 m/s.

For the resulting optimal design the effect of changing the position of the design point in the map has been studied by keeping tip speed and disc loading constant and only varying the C_p scale factor. Since the propeller efficiency is fairly constant around the design point the resulting fuel burn is insensitive to design point position as long as it is positioned within the high efficiency region.

In Figure 15 and 16 the C_p and J for the propeller during climb and cruise is indicated for the minimal fuel consumption design established above. Note that during the operation the Mach number changes and therefore the maps change. The maps shown here are simply included to give an indication of the propeller performance throughout the mission.

Within these calculations the rotational speed at low altitudes is increased by 10 % in order to push the operating line down towards higher efficiencies.

Discussion and conclusions

Each of the two propeller performance

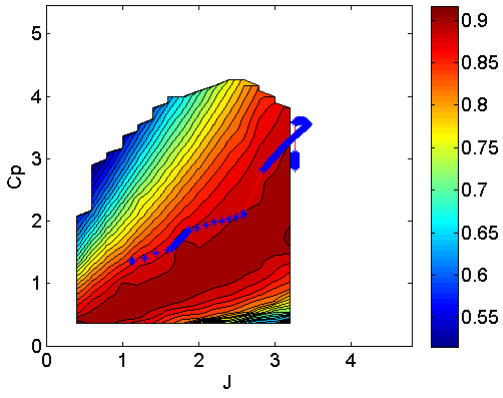

Figure 15: The operating line for the climb and cruise phase indicated in the map for low Mach numbers

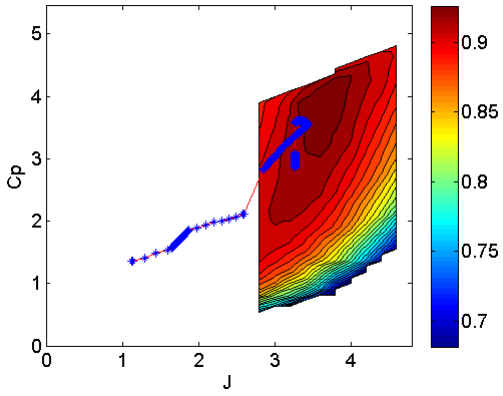

Figure 16: The operating line for the climb and cruise phase indicated in the map for Mach 0.8

calculation methods, using map modifications to reflect counter rotating propellers, have its benefits as well as drawbacks. If the map with constant scaling is used the design space is limited and only a certain range of disc loading can be evaluated. With the free scaling of the map to represent propellers designed for different disc loading, the design space that can be explored is much larger. With the free scaling method the efficiency is the same in the design point for both low and high disc loadings. This assumption is likely to overestimate the efficiency for high disc loadings since higher disc loadings do give higher velocities and thus more compressibility losses. Still, the two design methods using the counter rotating maps do generate similar trends with similar size propellers for the optimal design and similar fuel burn figures.

If the original single rotating map is used to represent counter rotating propellers the trends are significantly changed and are viewed to be unphysical. The optimal size propeller is closer to 4.5 m rather than 3.5 meters. The trends also show an increasing fuel consumption with decreasing tip speed which is not the case for the map where most of the swirl losses have been removed. The difference in mission fuel consumption between the two maps used for the optimal design is around 8 %. Note that this does not mean that a single rotating propeller would be 8 % less fuel efficient than an engine with counter rotating setup. The weight estimate still represents a substantially heavier counter rotating propeller.

Of the propeller performance representations studied here, either of the two maps with most swirl removed is worth developing. The constant scaling map might be extended towards higher coefficients of power. Another option is to introduce a loss factor for higher disc loadings if the free scale method is used. Since the engine weight and propeller module weight are shown to have significant impact on the optimal design of the propellers, it would be worth while to improve the propeller module weight modelling by further mechanical analysis.

References

[1] Flight international, 2007. ''Whatever happened to propfans''.

[2] Larsson, L., Avellán, R., and Grönstedt, T., 2011. ''Mission optimization of the geared turbofan engine''. *ISABE-2011-1314*.

[3] Hendricks, E. S., 2011. ''Development of an open rotor cycle model in NPSS using a multi-design point approach''. GT2011-46694, ASME.

[4] Bellocq, P., Sethi, V., Cerasi, L., Ahlefelder, S., Singh, R., and Tantot, N., 2010. ''Advanced open rotor performance modelling for multidisciplinary optimization assessments''. GT2010-22963, ASME.

[5] Seitz, A., Schmitt, D., and Donnerhack, S., 2011. ''Emission comparison of turbofan and open rotor engines under special consideration of aircraft and mission design aspects''. *Aeronautical Journal,* ***115***(1168), pp. 351--360.

[6] Baum, J., Dumais, P., Mayo, M., Metzger, F., Shenkman, A., and Walker, G., 1978. ''Prop-fan data support study''. *NASA-CR-152141*.

[7] Delano, J. B., and Crigler, J. L., 1953. ''Compressible-flow solutions for the actuator disk''. *NACA RM L53A07*.

[8] Hoff, G., 1990. ''Experimental performance and acoustic investigation of modern, counterrotating blade concepts''. *NASA Contractor Report 185158*.

[9] Avellán, R., and Grönstedt, T., 2007. ''Preliminary design of subsonic transport aircraft engines''. *ISABE 2007-1195*.

[10] Grönstedt, T., 2000. ''Development of methods for analysis and optimization of complex jet engine systems''. PhD thesis, Chalmers University of Technology.

[11] Kyprianidis, K. G., Au, D., Ogaji, S. O., and Grönstedt, T., 2009. ''Low pressure system component advancements and ist impact on future turbofan engine emissions''. *ISABE 2009-1276*.

[12] Isight 3.5. www.simulia.com.

Appendix 1

Propulsive efficiency

Net thrust: $T = \dot{m}(v_e - v_0)$

Mass flow: $\dot{m} = \rho A v_d$

Flow velocity at disc according to actuator disc theory:

$v_d = \frac{v_e + v_o}{2}$

$T = \rho A(\frac{v_e+v_0}{2})(v_e - v_0) = \frac{\rho A}{2}(v_e^2 - v_0^2)$

Propeller thrust: $T = C_t \rho n^2 D^4$

Advance ratio: $J = \frac{v_o}{nD}$

$C_t \rho \frac{v_0^2}{J^2} D^2 = \frac{\rho A}{2}(v_e^2 - v_0^2)$

Annulus area: $A = D^2 \frac{\pi}{4}(1 - htr^2)$

$C_t \rho \frac{v_0^2}{J^2} D^2 = \frac{\rho D^2}{2} \frac{\pi}{4}(1 - htr^2)(v_e^2 - v_0^2)$

$\frac{v_e}{v_0} = \sqrt{1 + \frac{C_t 8}{J^2 \pi (1 - htr^2)}}$

Propulsive efficiency: $\eta_p = \frac{2}{1 + \frac{v_e}{v_0}}$

$\eta_p = \frac{2}{1 + \sqrt{1 + \frac{C_t 8}{J^2 \pi (1 - htr^2)}}}$

Swirl losses

Power in tangential direction:

$\dot{w}_t = \frac{\dot{m} v_t^2}{2} = \frac{\dot{m} v_{ax}^2 \tan^2 \Theta}{2}$

Propeller mass flow:

$\dot{m} = \rho v_{ax} A = \rho v_{ax} D^2 \frac{\pi}{4}(1 - htr^2)$

$\dot{w}_t = \frac{\rho D^2 \pi (1 - htr^2) v_{ax}^3 \tan^2 \Theta}{8}$

Axial velocity:

$v_{ax} = v_0 + \Delta v = v_0(1 + \frac{\Delta v}{v_0})$

$\dot{w}_t = \frac{\rho D^2 \pi (1 - htr^2) v_0^3 (1 + \frac{\Delta v}{v_0})^3 \tan^2 \Theta}{8}$

Input power:

$P = c_p \rho n^3 D^5$

$SwirlLoss = \frac{\dot{w}_t}{P} = \frac{v_0^3}{n^3 D^3} \frac{\tan^2 \Theta (1 + \frac{\Delta v}{v_0})^3 \pi (1 - htr^2)}{c_p 8}$

$SwirlLoss = \frac{\pi (1 - htr^2)}{8} \frac{J^3 (1 + \frac{\Delta v}{v_0})^3 \tan^2 \Theta}{C_p}$